Effect of antiferromagnetic transition on the optical-absorption edge in MnO, α-MnS, and CoO†

H-h. Chou and H. Y. Fan
Department of Physics, Purdue University, West Lafayette, Indiana 47907
(Received 14 January 1974)

The effect of the magnetic transition on the optical-absorption edge has been studied for three antiferromagnetic crystals, MnO, α-MnS, and CoO. MnO shows a red shift, whereas α-MnS and CoO show a blue shift. The observations can be satisfactorily explained by a model which attributes the absorption edge to electron transitions from the magnetic ions to the conduction band. In the process, the electrons are localized around the ions excited. The lattice distortion and the changes in magnetic interactions are both significant for the effect.

I. INTRODUCTION

The effect of the magnetic transition on the optical-absorption edge has been studied previously for two antiferromagnetic crystals. Both $NaCrS_2$ (Ref. 1) and EuTe (Ref. 2) showed a shift to higher energy, blue shift, as the temperature was decreased below the Neél temperature T_N. The absorption edge in $NaCrS_2$ was attributed to transitions from the valence band to a localized energy level of the magnetic ions. In the case of EuTe, the observed edge was assumed to be associated with valence-band–conduction-band transitions. The effect of the ferromagnetic transition has been studied in seven crystals. For the Eu chalcogenides[2,3] EuO, EuS, and EuSe and the chromium chalcogenide spinels $CdCr_2Se_4$,[4] $HgCr_2S_4$,[5] and $HgCr_2Se_4$,[6] the edge shifted to a lower energy, red shift, when the temperature was decreased below the Curie temperature T_C. The absorption edge was attributed to valence-band–conduction-band transitions; transitions between localized energy levels of two neighboring magnetic ions was also considered for EuSe.[3] A blue shift was observed in the ferromagnetic spinel $CdCr_2S_4$,[3] the absorption edge was attributed to valence-band–conduction-band transitions. However, magneto-optic Kerr-effect studies[7] indicated that the edge associated with such transitions has actually a red shift and that the observed edge with blue shift is associated with an excitation band of magnetic ions which narrows with decreasing temperature. The edge shift in the ferromagnetic crystals has been variously interpreted as a lowering of the conduction band due to the exchange interaction with magnetic ions,[8] a change of energy separation between the conduction band and valence band as a result of lattice deformation produced by magneto-elastic coupling,[9] and a change of the excitation energy of a magnetic ion due to the spin ordering of neighboring ions.[3]

We have studied the effect of magnetic transition on the optical-absorption edge for three fcc antiferromagnetic crystals, MnO, α-MnS, and CoO. MnO is found to show a red shift, whereas a blue shift is observed in α-MnS and CoO. On the basis of reflection spectra measurements, Powell and Spicer[10] suggested that the absorption edge of CoO may be associated with transitions from a localized state of the magnetic ions to the conduction band or transitions from the valence band to the magnetic ions. By considering the available data for various magnetic crystals, Adler and Feinleib[11] suggested that localized-state–conduction-band transitions are responsible for the absorption edges in MnO and CoO. For α-MnS, Huffman and Wild[12] interpreted the observed absorption edge as valence-band–localized-state transitions. The shifts observed in our measurements provide information about the nature of transitions giving the observed edge and the mechanisms causing the edge shift.

II. EXPERIMENTAL RESULTS

Single crystals of MnO and CoO used in this work were cut from flame-fusion-grown Boules.[13] Single crystals of α-MnS were grown in our laboratory by the chemical-transport method with iodine as the carrier.[14] Specimens with a thickness of ~10 μ were used. The spectra were measured with an E-1 monochromator. Various filters were used to eliminate scattered light of long wavelengths. The detection system consisted of an S-5 response, RCA 1P28 photomuliplier, and a phase-sensitive amplifier.

Absorption bands observed in these crystals on the long-wavelength side of the sharply rising strong absorption have been interpreted as the excitation of d electrons localized around magnetic ions.[15,16] The valence band is derived mainly from $2p$ orbitals of halogen ions and is filled with $2p$ electrons and $4s$ electrons of magnetic ions. The conduction band is derived largely from $4s$ orbitals of magnetic ions. Band calculations[17,18] and vari-

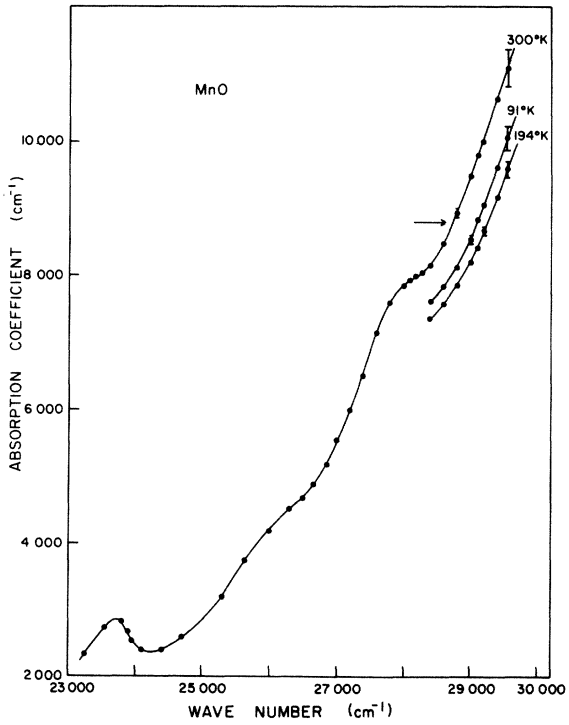

FIG. 1. Absorption coefficient vs wave number of radiation for MnO at three temperatures. Some error bars are shown for points with significant experimental uncertainty. The experimental uncertainty becomes very small with decreasing absorption. The level of absorption assumed to correspond to $h\nu_g$ is indicated by an arrow

ous experimental studies indicate that the energy gap between the two bands in these crystals is $\gtrsim 5$ eV, which is much higher than the photon energy of the sharply rising strong absorption. The $3d^{n+1}$ level of magnetic ions is estimated to be much higher than the normal levels $3d^n$ of magnetic ions in MnO (Ref. 19) and CoO.[11,19] The $3d^n$ levels lie above the valence band in the two crystals[20] as well as in α-MnS.[21] Electron transitions between two magnetic ions and transitions from the valence band to magnetic ions occur at photon energies much higher than the observed threshold of strong absorption. These considerations lead to the conclusion that the observed absorption edge in MnO and CoO is associated with electron transitions from magnetic ions to the conduction band. It seems reasonable that this conclusion applies also to α-MnS although contradictory evidence has been reported[22] regarding the energy of $3d^n$ levels relative to the valence band.

The magnetic transition in these crystals is accompanied by a crystallographic phase transition. From a cubic structure in the paramagnetic phase, MnO and α-MnS transform to a trigonal structure, whereas CoO transforms to a tetragonal structure in the antiferromagnetic phase. Our measurements did not reveal any dependence of the absorption edge on the polarization of radiation. Figures 1–3 show the absorption spectra of the three crystals for a few temperatures. An arrow indicates the absorption level which corresponds to the photon energy denoted by $h\nu_g$ and referred to as the absorption edge. The temperature variations of absorption edge for the three materials are shown in Fig. 4. The curve for MnO shows that the magnetic ordering produces a red shift which occurs near $T_N = 116$ °K, whereas the curve for α-MnS shows clearly a blue shift near $T_N = 160$ °K. For CoO, there is also a blue shift indicated by a change of slope near $T_N \sim 292$ °K. The dashed curve for MnO is obtained by extrapolating the data for $T > 200$ °K according to a T^2 variation. Such a temperature dependence is characteristic of normal semiconductors[23] at temperatures below the Debye temperature, ~510 °K for MnO. The difference between the extrapolation and the measured curve represents the effect of magnetic ordering. It should be noted that the dashed curve involves the effect of experimental uncertainty of the data used for extrapolation. The Debye temperature of α-MnS is in the range (200–300)°K.[12] The extrapola-

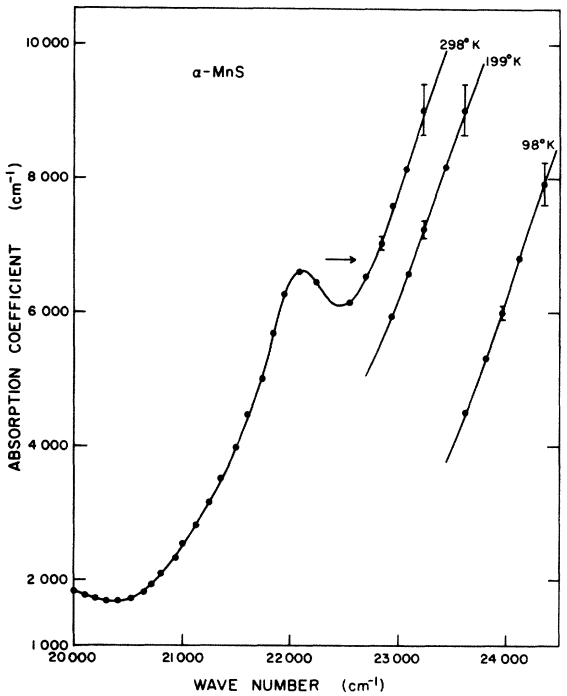

FIG. 2. Absorption coefficient vs wave number of radiation for α-MnS at three temperatures. Some error bars are shown for points with significant experimental uncertainty. The experimental uncertainty becomes very small with decreasing absorption. The level of absorption assumed to correspond to $h\nu_g$ is indicated by an arrow.

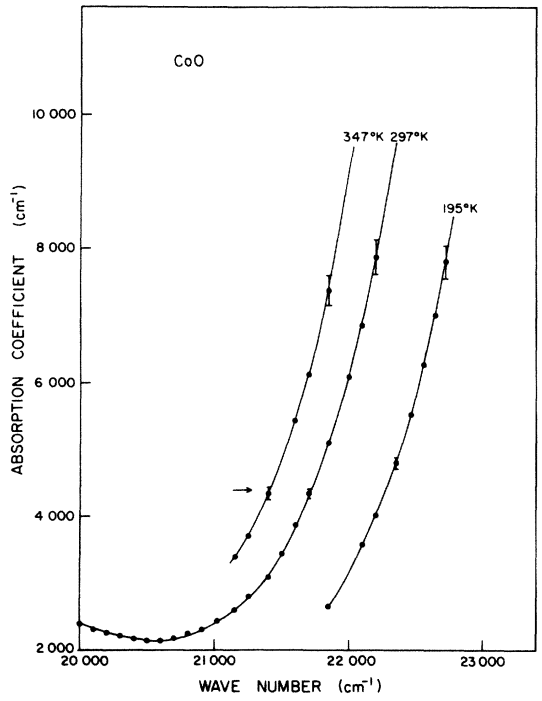

FIG. 3. Absorption coefficient vs wave number of radiation for CoO at three temperatures. Some error bars are shown for points with significant experimental uncertainty. The experimental uncertainty becomes very small with decreasing absorption. The level of absorption assumed to correspond to $h\nu_g$ is indicated by an arrow.

tion is made to be linear down to 100 °K, followed by a T^2 dependence at lower temperatures. The extrapolation in this case is less reliable since the range of extrapolation is larger due to the higher transition temperature. The extrapolation for CoO should be regarded as having the largest uncertainty. The approximate values of $\Delta h\nu_g = h\nu_g(0\ ^\circ\mathrm{K}) - h\nu_g(T \gg T_N)$ are listed in Table I.

In order to investigate the effect of crystallographic distortion, measurements were made for the paramagnetic phase of MnO with applied unilateral strain. The sample had its length along a ⟨111⟩ direction and it was cemented to a piece of aluminum at the two ends. The sample experienced a uniaxial extension as the temperature was raised. The strain is similar to the distortion associated with magnetic transition, except for that a contraction along a ⟨111⟩ direction is involved in the transition. The absorption was measured with radiation polarized parallel or transverse to the ⟨111⟩ direction. Curves of $h\nu_g$ as a function of temperature were obtained before and after the sample was cemented to the metal support. The results are plotted in Fig. 5. A strain $\Delta l/l$ due to the difference in thermal expansion between MnO and alu-

TABLE I. Experimentally obtained $\Delta h\nu_g$ and theoretically calculated $\Delta(E_1)_M$ are given in the first two rows. Theoretically calculated effect $[\Delta(E_1)_D + \Delta(E_2)_D]$ of crystallographic distortion and the required effect $\Delta(E_2)_M$ of magnetic interaction of the excited electron are given for the free-electron and localized-electron models.

ΔE (cm^{-1})		MnO	α-MnS	CoO
$\Delta h\nu_g$(expt.)		−500 ± 50	~780	~200
$\Delta(E_1)_M$		+200	+240	+40
Free electron	$\Delta(E_1)_D + \Delta(E_2)_D$	+240	+260	+910
	$\Delta(E_2)_M$	−900(< 0)	+280	−750(< 0)
Localized electron	$\Delta(E_1)_D + \Delta(E_2)_D$	170 ± 190	~250	~910
	$\Delta(E_2)_M$	−870 ± 240	+290	~−750

minum produces a volume dilatation

$$\Delta V/V = (1 - 2\sigma)(\Delta l/l) \qquad (1a)$$

and a trigonal distortion

$$\delta = \tfrac{2}{3}(1 - 1/\sigma)(\Delta l/l)\ , \qquad (1b)$$

where σ is the Poisson ratio and δ is the angle between an axis of the trigonal cell and the corre-

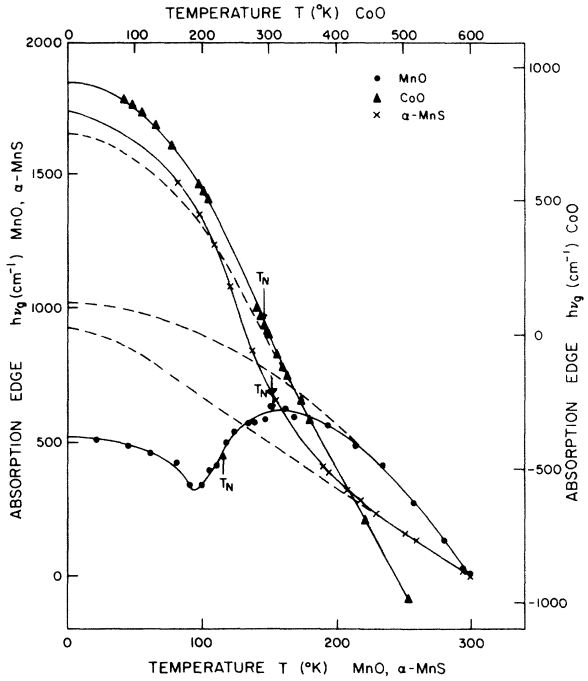

FIG. 4. Absorption edge $h\nu_g$ as a function of temperature for MnO, α-MnS, and CoO is shown by the solid curves. The dashed curve in each case shows the extrapolation of $h\nu_g$ from temperatures above the Neél temperature T_N. The maximum uncertainty in $h\nu_g$ is ± 25 cm^{-1}, being smaller for the points at higher temperature. The uncertainty is progressively smaller in the order MnO, α-MnS, and CoO as the absorption edge is steeper in that order.

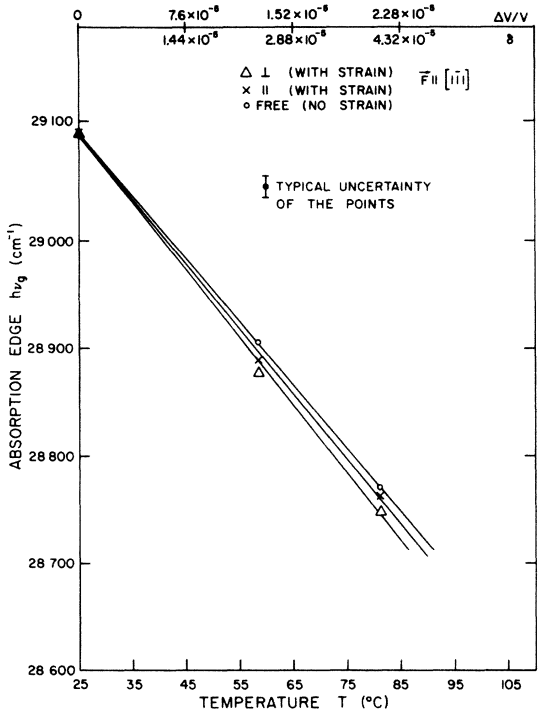

FIG. 5. Absorption edge $h\nu_g$ of MnO as a function of temperature in the paramagnetic phase. The thin sample had (110) interfaces. The data points O were obtained with the sample free to expand. The data points × and Δ were obtained with the sample cemented at the two ends. The points × and Δ are for radiation polarized parallel to $[1\bar{1}1]$ and $[1\bar{1}\bar{2}]$, respectively.

sponding cubic axis. The estimated values of $\Delta V/V$ and δ are indicated on the horizontal axis of Fig. 5.

III. THEORY

The photon energy at the absorption edge may be considered to consist of an energy change E_1 of the magnetic ion and the energy E_2 of the carrier produced. The effect of magnetic transition on the absorption edge is $\Delta h\nu_g = \Delta E_1 + \Delta E_2$. Each of the two quantities ΔE_1 and ΔE_2 maybe separated into the effect of crystallographic distortion ΔE_D and the effect of magnetic interaction ΔE_M. We shall consider first the energy of a magnetic ion.

A. Magnetic ion

1. Effect of crystallographic distortion

We have to consider the states of the Mn and Co ions in the paramagnetic and antiferromagnetic phases of the crystal. The spin-orbit interaction of the electrons will be neglected as is usually done.

Co^{++} *ion.* Consider a free ion in the zero-order approximation where the electrostatic interaction among the $3d$ electrons is neglected. The five electronic orbitals may be chosen as

$$\begin{aligned}
&\xi(t_{2g}, e_g) = (i/\sqrt{2})(d_{+1} + d_{-1}) ,\\
&\eta(t_{2g}, e_g) = (-1/\sqrt{2})(d_{+1} - d_{-1}) ,\\
&\xi(t_{2g}, b_{2g}) = (i/\sqrt{2})(d_{+2} - d_{-2}) ,\\
&\epsilon(e_g, b_{1g}) = (1/\sqrt{2})(d_{+2} + d_{-2}) ,\\
&\theta(e_g, a_{1g}) = d_0 ,
\end{aligned} \tag{2}$$

where the representation in the cubic symmetry group and the representation in the tetragonal symmetry group are indicated consecutively in the bracket following the notation. For the ion with seven $3d$ electrons and $S = \frac{3}{2}$, there are 40 degenerate states. In terms of representations of the cubic-symmetry group, these states may be divided into four groups, of which two have T_{1g}, one has A_{2g}, and one has T_{2g} representation.[24]

Consider now Co^{++} in cubic CoO. The cubic crystalline field splits the energy for the five electronic wave functions (2) into two levels $\epsilon(t_{2g})$ and $\epsilon(e_g)$. The crystalline field together with the electrostatic interaction among the $3d$ electrons splits the degeneracy of the four groups of ion states. According to Pratt and Coelho,[15] the ground state has a three-dimensional T_{1g} representation with fourfold spin degeneracy. Using the wave function given by Pratt and Coelho,[15] we calculate the ground-state energy to be

$$E(^4T_{1g}) = 4.94\epsilon(t_{2g}) + 2.06\epsilon(e_g) + 21A + 14C - 40.9B , \tag{3}$$

where the last three terms with the Racah constants A, B, and C represent the effect of mutual repulsion of the electrons.

The crystalline field in the antiferromagnetic phase of CoO has tetragonal symmetry D_{4h}. Treating the effect of change in crystalline field from that of the cubic phase as perturbation, we find the $^4T_{1g}$ state to be split into A_{2g} and E_g with the energies

$$E(^4A_{2g}) - E(^4T_{1g}) = -1.64D_s + 3.08D_t + (7D_d - 0.74\Delta_d)(\Delta V/V) , \tag{4a}$$

and

$$E(^4E_g) - E(^4T_{1g}) = 0.82D_s - 1.55D_t + (7D_d - 0.74\Delta_d)(\Delta V/V) . \tag{4b}$$

The first two terms with parameters[24] D_s and D_t represent the effect of symmetry distortion and the term with $\Delta V/V$ represents the effect of dilatation. D_d pertains to $\frac{1}{5}[\epsilon(a_{1g}) + \epsilon(a_{2g}) + \epsilon(b_{2g}) + 2\epsilon(e_g)]$, while Δ_d pertains to $[\epsilon(e_g) - \epsilon(t_{2g})]$. In the cubic phase, there are excited states $^4T_{1g}$ and $^4T_{2g}$ and the ground state is $^4T_{1g}$. Each $^4T_{1g}$ and the $^4A_{2g}$ are split when the crystal becomes tetragonal. Consequently, ab-

sorption peaks corresponding to $({}^4T_{1g} \rightarrow {}^4T_{1g})$ and $({}^4T_{1g} \rightarrow {}^4T_{2g})$ transitions are each split. The splitting can be shown to be $(-5.45D_s + 0.87D_t)$ for $({}^4T_{1g} \rightarrow {}^4T_{1g})$ and $(-8.75D_t)$ for $({}^4T_{1g} \rightarrow {}^4T_{2g})$. From experimentally determined splittings of 530 cm^{-1} for $({}^4T_{1g} \rightarrow {}^4T_{1g})$ and 1080 cm^{-1} for $({}^4T_{1g} \rightarrow {}^4T_{2g})$[15], we get $D_s = -117$ cm^{-1} and $D_t = -123$ cm^{-1}. Using these values, we see that the ${}^4A_{2g}$ state has lower energy than the ${}^4E_g$ state in tetragonal phase.

Co^{+++} *ion.* Since $\Delta S = 0$ for an optical transition, the excitation of a Co^{++} with $S = \frac{3}{2}$ may lead to a Co^{+++} with $S = \frac{3}{2} \pm \frac{1}{2}$ depending upon the spin of the excited electron. According to Griffith,[25] the lowest energy for an ion of d^6 configuration is

in case $S = 1$,

$$E({}^3T_{1g}) = 5\epsilon(t_{2g}) + \epsilon(e_g) + 15A - 30B + 12C \ , \tag{5}$$

in case $S = 2$,

$$E({}^5T_{2g}) = 4\epsilon(t_{2g}) + 2\epsilon(e_g) + 15A - 35B + 7C \ .$$

The ${}^3T_{1g}$ state corresponds to the $t_{2g}^5 e_g$ configuration and the ${}^5T_{2g}$ state corresponds to the $t_{2g}^4 e_g^2$ configuration. The difference of the two orbital energies $[\epsilon(e_g) - \epsilon(t_{2g})]$ is 9420 cm^{-1} for Co^{++} in CoO. The value appropriate for an excited Co^{+++} may be somewhat different but it is clear that ${}^5T_{2g}$ is the state of lower energy in view of[26] $B = 1065$ cm^{-1} and $C = 5120$ cm^{-1}.

For the antiferromagnetic phase, a treatment analogous to that used in the previous case gives

$$E({}^5E_g) - E({}^5T_{2g}) = -D_s + 1.67D_t + (6D_d - 0.4\Delta_d)(\Delta V/V) \ , \tag{6a}$$

$$E({}^5A_{2g}) - E({}^5T_{2g}) = 2D_s - 3.33D_t + (6D_d - 0.4\Delta_d)(\Delta V/V) \tag{6b}$$

for the two states split from the ${}^5T_{2g}$ state of the cubic phase. With the values of D_s and D_t given before, we see that $E({}^5E_g) < E({}^5A_{2g})$. Combining (6a) and (4a) we get the effect of lattice distortion on the change of ion energy involved in an optical transition:

$$\Delta(E_1)_D = 0.64D_s - 1.4D_t - (D_d - 0.34\Delta_d)(\Delta V/V) \equiv 0.64D_s - 1.41D_t - D(\Delta V/V) \ . \tag{7}$$

Mn^{++} *ion.* The ground state of Mn^{++} in MnO is ${}^6A_{1g}$,[15] which is associated with $t_{2g}^3 e_g^2$ in zeroth order. The energy of the ground state is[25]

$$E({}^6A_{1g}) = 3\epsilon(t_{2g}) + 2\epsilon(e_g) + 10A - 35B \ . \tag{8}$$

The crystalline field in the antiferromagnetic phase of MnO has a trigonal D_{3d} symmetry group. The ground state does not split under trigonal distortion, having the A_{1g} representation of the D_{3d} group. The energy can be shown to be

$$E({}^6A_{1g})_{AF} - E({}^6A_{1g})_{PM} = 5D_d(\Delta V/V) \ , \tag{9}$$

where $D_d(\Delta V/V)$ represents the shift of $\frac{1}{5}[3\epsilon(t_{2g}) + 2\epsilon(e_g)]$ due to volume contraction associated with distortion.

Mn^{+++} *ion.* Mn^{+++} resulting from optical excitation of a Mn^{++} ion with $S = \frac{5}{2}$ has a spin $S = 2$ with a lowest energy[25]

$$E({}^5E_g) = 3\epsilon'(t_{2g}) + \epsilon'(e_g) + 6A - 21B \ . \tag{10}$$

The state ${}^5E_g$ corresponds to the $t_{2g}^3 e_g$ configuration. The state is not split by the crystalline distortion of the antiferromagnetic phase, having the E_g representation of the D_{3d} group, with an energy

$$E({}^5E_g)_{AF} - E({}^5E_g)_{PM} = (4D_d - 0.6\Delta_d)\Delta V/V \ . \tag{11}$$

We get by subtracting (9) from (11),

$$\Delta(E_1)_D = -(D_d + 0.6\Delta_d)\Delta V/V \equiv -D\Delta V/V \tag{12}$$

2. *Effect of magnetic interaction*

The exchange interaction between a magnetic ion and its neighbors contributes to ΔE_1. The effect has been considered for the ferromagnetic EuSe (Ref. 3) and antiferromagnetic $NaCrS_2$.[1] We are interested in magnetic ions with an unfilled $3d$ shell. All electrons have spins along the direction of the ion spin and only the electrons with unpaired spins are involved in the interaction. The interaction of a magnetic ion with the next-nearest magnetic neighbors involves 180° superexchange and can be written

$$2\sum_m \sum_{i,j(m)} J_{i,j(m)} \langle \vec{s}_i \cdot \vec{s}_j \rangle = 2\sum_m \frac{\langle \vec{S} \cdot \vec{S} \rangle_m}{4SS_m} \times \sum_{i,j(m)} J_{i,j(m)} \ , \tag{13}$$

where m is an index of the neighbor, i is an index for orbitals with unpaired electrons of the ion and $j(m)$ is that for the mth neighbor, J is the exchange integral, and $\vec{s}$ and $\vec{S}$ are, respectively, electron spin and ion spin. Since the time average or correlation function $\langle \vec{S} \cdot \vec{S} \rangle_m$ is independent of m for next nearest neighbors we can write the interaction as

$$2\langle \vec{S} \cdot \vec{S}_2 \rangle \sum_m \sum_{i,j(m)} \frac{J_{i,j(m)}}{4SS_m} \ . \tag{14}$$

$\vec{S}_2$ is the spin of a next nearest magnetic neighbor. In a treatment of 180° superexchange in MnF_2, only e orbitals were considered.[27] We shall adopt

this approximation. With all the neighbors in the ground state, it can be shown that for the next nearest neighbors

$$z_2 J_2 \equiv \sum_m \sum_{i,j(m)} \frac{J_{i,j(m)}}{4SS_m} \propto \frac{\Delta_e(\Delta_e)_2}{S} . \quad (15)$$

z_2 is the number of neighbors. Δ_e is the number of unpaired electrons in the e_g orbitals involved in the ion state. For Co^{++}, two zeroth-order wave functions are involved and Δ_e is weighted accordingly:

$$\Delta_e = 2\times 0.97^2 + 1\times 0.25^2 = 1.94.$$

The interaction with nearest magnetic neighbors consists of 90° superexchange. In the antiferromagnetic phase, there are six neighbors on a plane passing through a magnetic ion, which has ions of similarly oriented (+) spins. The other six neighbors are on the two adjacent planes which contain ions of opposite spins (−). It has been shown[27] that interactions between e orbitals and t orbitals are most important for 90° superexchange. We get analogously as for the above case that the interaction with nearest neighbors is

$$J_{1+} z_1 \langle \vec{S}\cdot\vec{S}_{1+}\rangle + J_{1-} z_1 \langle \vec{S}\cdot\vec{S}_{1-}\rangle ,$$

where

$$\tfrac{1}{2} z_1 J_{1\pm} \equiv \sum_{m\pm} \sum_j \frac{J_{ij(m\pm)}}{4SS_{m\pm}} \propto \frac{\Delta_t(\Delta_e)_1 + \Delta_e(\Delta_t)_1}{S} , \quad (16)$$

z being the number of neighbors. Similar to Δ_e, Δ_t refers to t orbitals. The subscript 1 is used to indicate nearest magnetic neighbors. $J_{1\pm}$ are for the two groups of ions which have different separations from the central ion.

The contribution of the superexchange to E_1 is

$$(E_1)_M = -2z_2 J_2 \langle \vec{S}\cdot\vec{S}_2\rangle \left(\frac{\Delta_e'}{\Delta_e} - 1\right) + z_1[J_{1+}\langle \vec{S}\cdot\vec{S}_{1+}\rangle + J_{1-}\langle \vec{S}\cdot\vec{S}_{1-}\rangle] \times \left(\frac{\Delta_t'(\Delta_e)_1 + \Delta_e'(\Delta_t)_1}{\Delta_t(\Delta_e)_1 + \Delta_e(\Delta_t)_1} - 1\right) , \quad (17)$$

where Δ_e' and Δ_t' refer to the ion after optical excitation. We shall use the approximation $J_{1+} \sim J_{1-}$ and neglect small variations of J_1 and J_2 with phase transition. The effect

$$\Delta(E_1)_M = (E_1)_M^{AF} - (E_1)_M^{PM} \quad (18)$$

is due to differences in the spin-correlation functions of the two phases. In the antiferromagnetic phase, $\langle \vec{S}\cdot\vec{S}_{1+}\rangle$ and $\langle \vec{S}\cdot\vec{S}_{1-}\rangle$ have opposite signs, and the contribution of nearest neighbors to $(E_1)_M$ can be obviously expected to be small.

B. Excited carrier

1. *Effect of crystallographic distortion*

Lattice distortion associated with magnetic transition may affect the energy of the excited electron. We express the contribution to the effect of magnetic transition by two parameters D_v and D_δ:

$$\Delta(E_2)_D = D_v(\Delta V/V) + D_\delta \delta , \quad (19)$$

where D_v represents the effect of volume change and D_δ represents the effect of symmetry distortion δ which may give through splitting additional change of the lowest energy. For a band edge at $\vec{k}=0$, a symmetry distortion has no first-order effect for a conduction electron near the band edge. The effect of the symmetry distortion may be significant for a conduction electron which becomes localized.

2. *Effect of magnetic interaction*

Free electron. The exchange interaction of conduction electrons and magnetic ions has been treated by Rys *et al.*[8] For temperatures much above the transition temperature, the expression given for the energy shift of the conduction band is

$$[\Delta\epsilon(\vec{k})]_{T\gg T_N} = \frac{S(S+1)}{4N} \times \sum_q \frac{|J(\vec{k},\vec{k}-\vec{q})|^2}{\epsilon(\vec{k}) - \epsilon(\vec{k}-\vec{q})} \quad (20)$$

in second order. The interaction has no effect in first order. The second-order effect consists of two parts, static interaction in which the spin system remains unchanged and dynamic interaction involving excitations of the spin system in the intermediate state of second-order perturbation. Let $\Delta_s''\epsilon(\vec{k})$ and $\Delta_d''\epsilon(\vec{k})$ be, respectively, the second-order shifts of the energy level $\epsilon(\vec{k})$ in the conduction band due to the two interactions. For temperatures below the transition temperature, $\Delta_d''\epsilon(\vec{k})$ just compensates a part of the first-order shift $\Delta'\epsilon(\vec{k})$, in ferromagnets. For antiferromagnets, there is no first-order shift. The expression

$$[\Delta_s''\epsilon(\vec{k})]_{T\ll T_N} = \frac{S_z^2}{4} \sum_{\vec{q}} \frac{|J(\vec{k},\vec{k}-\vec{Q}-\vec{D})|^2}{\epsilon(\vec{k}) - \epsilon(\vec{k}-\vec{Q}-\vec{D})} \quad (21)$$

is given for type-2 antiferromagnets. For $T \ll T_N$, $|S_z| \sim S$. We add the effect of dynamic interaction:

$$[\Delta_d''\epsilon(\vec{k})]_{T\ll T_N} = \frac{S}{N} \sum_{\vec{q}} \frac{|J(\vec{k},\vec{k}-\vec{q})|^2}{4}$$

$$\times (u_{\vec{q}}+v_{\vec{q}})^2\times\left(\frac{n_{\vec{q}}+1}{\epsilon(\vec{k})-\epsilon(\vec{k}+\vec{q})-\hbar\omega_{\vec{q}}}+\frac{n_{\vec{q}}}{\epsilon(\vec{k})-\epsilon(\vec{k}-\vec{q})+\hbar\omega_{\vec{q}}}\right). \quad (22)$$

In the above expressions, $\vec{Q}$ is a reciprocal-lattice vector in the paramagnetic phase, $\vec{D}=(\pi/a)\,(1,1,1)$ is normal to the set of planes of similarly oriented magnetic ions, N is the number of magnetic ions in the crystal, S is the spin of a magnetic ion, $\hbar\omega_{\vec{q}}$ is the energy of a magnon with wave vector $\vec{q}$, $n_{\vec{q}}$ is the occupancy quantum number of the magnon, $\pm u_{\vec{q}}^2$ is the change of z component of total spin of one sublattice, $\mp v_{\vec{q}}^2$ is the change of the other sublattice to an excited magnon, and J is the exchange integral between a conduction electron and a magnetic ion.

The edge of the conduction band in these crystals is at $\vec{k}=0$.[17,18] Taking $\epsilon(\vec{k})=\hbar^2k^2/2m^*$, we have $\hbar\omega_{\vec{q}}\ll|\epsilon(\vec{k})-\epsilon(\vec{k}-\vec{q})|$ at $\vec{k}\approx 0$; therefore we neglect $\hbar\omega_{\vec{q}}$ in (22). The notation $J_{\vec{q}}\equiv J(\vec{k},\vec{k}-\vec{q})$ will be used. Theoretical calculations[28] show that $|J_{\vec{q}}|^2$ decreases rapidly with increasing $|\vec{q}|$ outside of the first Brillouin zone, for s-type conduction electrons and for f electrons of a magnetic ion. The assumption $J_{\vec{q}}=J_0$ for

$$q\le |J_0|^{-2}\int_0^{\infty}|J_{\vec{q}}|^2\,d\vec{q}$$

and $J_{\vec{q}}=0$ for larger q has been used by Rys *et al.* We shall take $J_{\vec{q}}=J_0$ inside the first Brillouin zone and $J_{\vec{q}}=0$ outside, for the paramagnetic phase. For the antiferromagnetic phase, $J_{\vec{q}}=J_0$ is taken for the first two zones which correspond to the first zone of the paramagnetic phase. Combining (20)–(22), we get

$$\Delta(E_2)_M=[\epsilon(0)_{T\ll T_N}-\epsilon(0)_{T\gg T_N}]_{ex}=-\frac{|J_0|^2}{4}\frac{2m^*}{\hbar^2D^2}S^2-\frac{S}{4N}|J_0|^2\sum_{\vec{q}}\frac{2m^*}{\hbar^2q^2}(u_{\vec{q}}+v_{\vec{q}})^2(2n_{\vec{q}}+1)+|J_0|^2\frac{S(S+1)}{4N}\sum_{\vec{q}}\frac{2m^*}{\hbar^2q^2}. \quad (23)$$

Localized electron. In the usual effective-mass approximation, the envelope function of well-localized states extends over only a few lattice cells if $m^*\sim m$ as in the crystals of interest. Applicability of the approximation is questionable in such cases. We shall approximate the wave function of a localized state by a linear combination of orbitals of the central ion and the neighboring oxygen and magnetic ions. The $2p$ orbitals of oxygen ions (or $3p$ orbitals of sulphur ions) and the $4s$ orbital of the magnetic ions are included since the conduction band involves mainly these orbitals. We are interested in the lowest state of an ion with a localized electron which allows optical transition from the normal state of the ion, A_{1g} for Mn^{++} and T_{1g} for Co^{++}. This consideration prescribes allowed symmetry representations for the wave function of localized electron. We take $4p$ orbitals of the central ion for the linear combination because this orbital is associated with lowest energy among the orbitals which can give linear combinations satisfactory for the symmetry requirement.

We get three wave functions ψ_x, ψ_y, ψ_z, which form a three-dimensional representation T_{1u} of the symmetry group. The three wave functions can be expressed concisely as follows:

$$\begin{aligned}
\psi_x &= A(4p_x)_0+B[(p_x)_a+(p_x)_b]+C[(p_x)_c+(p_x)_d+(p_x)_e+(p_x)_f]\\
&\quad +D\{[(4s)_1+(4s)_2+(4s)_7+(4s)_8]-[(4s)_4+(4s)_5+(4s)_{10}+(4s)_{11}]\}+E[(4s)_I-(4s)_{II}],\\
\psi_y &= A(4p_y)_0+B[(p_y)_c+(p_y)_d]+C[(p_y)_e+(p_y)_f+(p_y)_a+(p_y)_b]\\
&\quad +D\{[(4s)_2+(4s)_3+(4s)_9+(4s)_{10}]-[(4s)_5+(4s)_6+(4s)_{12}+(4s)_7]\}+E[(4s)_{III}-(4s)_{IV}],\\
\psi_z &= A(4p_z)_0+B[(p_z)_e+(p_z)_f]+C[(p_z)_a+(p_z)_b+(p_z)_c+(p_z)_d]\\
&\quad +D\{[(4s)_3+(4s)_4+(4s)_{11}+(4s)_{12}]-[(4s)_6+(4s)_4+(4s)_8+(4s)_9]\}+E[(4s)_V-(4s)_{VI}].
\end{aligned} \quad (24)$$

The axes taken are the cubic edge of conventional unit cell.

A, B, C, D, E are coefficients. The subscript 0 denotes the central ion, $a, b, \ldots, f$ are indices of nearest halogen ions, $1, 2, \ldots, 12$ are indices of nearest magnetic ions, and $I, II, \ldots, VI$ are indices of next-nearest magnetic ions. For each wave function, the second term is a linear combination of p orbitals for two halogen ions situated along one of the three axes. The fourth term consists

of two linear combinations of 4s orbitals; the combination with positive sign is for ions which have positive coordinates along the axis and the other combination is for ions having negative coordinates along the axis.

The first-order magnetic-interaction energy does not vanish in the antiferromagnetic phase for a localized electron. It is given by

$$\Delta\epsilon = -\vec{s}\cdot\sum_i \vec{S}_i \left\langle \iint \psi^*(\vec{r}_1)\varphi_{3d}^*(\vec{r}_2-\vec{R}_i)\,\frac{e^2}{r_{12}}\,\varphi_{3d}(\vec{r}_1-\vec{R}_i)\,\psi(\vec{r}_2)\,d\vec{r}_1\,d\vec{r}_2 \right\rangle_{av} ,$$

where ψ and s are the spatial wave function and spin of localized electrons, i is the index of neighboring magnetic ions, φ_{3d} is an unpaired zero-order $3d$ wave function, and the weighted average over the unpaired $3d$ orbitals is denoted by $\langle\cdots\rangle_{av}$. The summation over i excludes the central ion since the interaction with the central ion does not vary with the temperature. For $T \gg T_N$, neighboring magnetic ions have little effect due to the randomness of their spins. In the antiferromagnetic phase, half of the nearest magnetic ions (indices 7–12) have spins parallel to that of the central ion and the other half (indices 1–6) have opposite spins. All the next-nearest magnetic ions have spins parallel to that of the central ion. The magnetic interaction with neighboring magnetic ions splits the threefold degeneracy of the localized state, leading to a singlet state and a doubly degenerate state. In the Mn compounds, the spin of the excited electron is parallel to the spin of the central ion. Since s-d exchange integrals are positive, the doubly degenerate state is lower in energy. The magnetic interaction lowers the energy by

$$\Delta E = \Delta(E_2)_M = -(2D^2 - E^2)SJ_{sd} , \qquad (25a)$$

where

$$J_{sd} \equiv \langle \iint \varphi_{4s}^*(\vec{r}_1)\varphi_{3d}^*(\vec{r}_2)(e^2/r_{12}) \times \varphi_{3d}(\vec{r}_1)\varphi_{4s}(\vec{r}_2)\,d\vec{r}_1\,d\vec{r}_2\rangle_{av}$$

and S is the magnitude of spin of a magnetic ion. In CoO, the spin of the excited electron is antiparallel to the spin of the central ion; the singlet state is lower in energy with

$$\Delta(E_2)_M = -(4D^2 + E^2)SJ_{sd} . \qquad (25b)$$

In (25a) and (25b), overlap of 4s orbitals with $3d$ orbitals of different magnetic ions are neglected.

IV. INTERPRETATION OF EXPERIMENTAL RESULTS

In view of (19) and (7) or (12), we may write

$$\begin{aligned}\Delta h\nu_g &= \Delta(E_1)_M + \Delta(E_2) + \Delta(E_1)_D + \Delta(E_2)_D \\ &= \Delta(E_1)_M + \Delta(E_2)_M + (D_v - D)(\Delta V/V) + D_6\delta \\ &\quad + (0.64D_s - 1.41D_t) .\end{aligned}$$

The last term is present only for CoO, $\Delta(E_1)_M$ is given by (18). $\Delta(E_2)_M$ is given by (23) if a free conduction electron is excited, and it is given by (25) if the excited electron is localized. In the paramagnetic phase, Mn^{++} is in the ${}^6A_{1g}$ state and Co^{++} is in the ${}^4T_{1g}$ state. At the absorption edge, the electron excited by optical transition is close to the conduction-band minimum which has A_1 representation of cubic group.[17,18] After an optical transition, Mn^{+++} has a E_g and Co^{+++} has a T_{2g} representation. The electric-dipole moment involved in an optical transition has a T_{1u} representation. Since $E_g \times A_1$ does not contain $T_{1u} = T_{1u} \times A_{1g}$, the transition is forbidden for the Mn compounds. For CoO, the transition is allowed or forbidden depending upon whether the representation of the conduction band is specifically A_{1u} or A_{1g}. Since the conduction band is supposed to consist mainly of 4s orbitals of magnetic ions, A_{1g} is the more likely representation, in which case the transition is also forbidden. Since all the crystals have inversion symmetry in the antiferromagnetic phase, the parity of a state is not changed by the phase transition, hence the transition under consideration is also forbidden in the antiferromagnetic phase. In the case of MnO, our strain measurements also provide an evidence against the excitation of free electrons. The edge of the conduction band and the state of Mn^{++} are nondegenerate. The degeneracy of Mn^{+++} involved is not split by the distortion of $\langle 111\rangle$ strain. In the hypothesis of free-electron excitations, we would have $D_6 = 0$ and

$$(\Delta h\nu_g)_{\parallel} = (\Delta h\nu_g)_{\perp} = (D_v - D)(\Delta V/V) .$$

The fact that the measured $(\Delta h\nu_g)_{\parallel}$ and $(\Delta h\nu_g)_{\perp}$ are different is against this hypothesis.

Despite these considerations, the absorption edge in MnO and CoO has been attributed to the excitation of electrons to the conduction band.[10,11,19] Let us examine first this hypothesis: We take the average of $(\Delta h\nu_g)_{\parallel}$ and $(\Delta h\nu_g)_{\perp}$ given by the strain measurements, which corresponds to $D_v - D = -9$ eV. This value is assumed for all three crystals. The values of $\Delta V/V$ due to the magnetic effect on the crystallographic structure at 0 °K are listed in Table II. The values of D_s, D_t for CoO have been quoted previously. The values of $[\Delta(E_1)_D$

TABLE II. Volume dilatation $\Delta V/V$ and symmetry distortion δ[a] associated with antiferromagnetic transition. Exchange integral J_1 and J_2 for nearest and next nearest neighbors, respectively, are also shown.

Parameters	MnO	α-MnS	CoO
J_1 (°K)	-10[b]	-7[b]	-6.9[c]
J_2 (°K)	-11[b]	-12.5[b]	-21.6[c]
$\Delta V/V$ (at 0 °K)	-3.3×10^{-3}[b]	-3.6×10^{-3}[b]	-1.2×10^{-2}[d]
δ (at 0 °K)	1.1×10^{-2}[b]	1.72×10^{-3}[b]	7.5×10^{-3}

[a] δ is expressed in terms of corner angle change $\pm\Delta$ for trigonal distortion and in terms of $\frac{2}{3}\epsilon_{zz}$ for tetragonal distortion. Corner angle: angle defined by two of the basis vectors of conventional unit cell. It is $\pi/2$ in fcc crystal.

[b] B. Morosin, Phys. Rev. B 1, 236 (1970).

[c] L. M. Corliss, N. Elliott, and J. M. Hastings, Phys. Rev. 104, 924 (1956).

[d] M. R. Daniel and A. P. Crakknell, Phys. Rev. 177, 932 (1969).

$+\Delta(E_2)_D]$ calculated with the values of (D_v-D), $\Delta V/V$, D_s, and D_t, are listed in the second row of Table I. The values of J_1 and J_2 are listed in Table II and the calculated values of $\Delta(E_1)_M$ are listed in Table I. The values of $(\Delta E_2)_M$ required to fit the observed $\Delta h\nu_g$ are listed in the fourth row. It is seen that $\Delta(E_2)_M<0$ is needed for MnO and CoO. On the other hand, theoretical calculations show that $\sum(u_{\vec{q}}+v_{\vec{q}})^2/q^2$ is smaller than $\sum 1/q^2$ by a factor of ~0.8 for fcc type-2 antiferromagnets. Since $(1/N)\sum 1/q^2 > 1/D^2$, (23) gives $\Delta(E_2)_M>0$. Therefore, the free-electron model is inconsistant with the experimental results for MnO and CoO even though the values of $\Delta(E_2)_M$ required for α-MnS may be fitted by (23) with reasonable value of m^* and J_0.

Consider the model where the optically excited electron is localized. In our strain measurement on MnO, the elongation was applied along a ⟨111⟩ direction. The triply degenerate state ψ_x, ψ_y, ψ_z is split into a singlet state ψ_1 and a doublet state ψ_2, ψ_3 as indicated in Fig. 6. Excitation to ψ_1 is allowed for radiation polarized perpendicular to the ⟨111⟩ direction, whereas excitations to ψ_2, ψ_3 are allowed for polarization along the ⟨111⟩ direction also. The difference between $(\Delta h\nu_g)_{\parallel}$ and $(\Delta h\nu_g)_{\perp}$ shows the ψ_1 state to be lower in energy. We have the relations

$$(\Delta h\nu_g)_{\perp}=(D_v-D)\Delta V/V+(D_\delta)_a\,\delta\ ,$$

$$(\Delta h\nu_g)_{\parallel}=(D_v-D)\Delta V/V+(D_\delta)_b\,\delta\ .$$

Perturbation treatment of symmetry distortion shows

$$\tfrac{1}{2}(D_\delta)_a\,\delta=-(D_\delta)_b\,\delta\ .$$

Using the above three relations, we get from the measured $(\Delta h\nu_g)_{\parallel}$ and $(\Delta h\nu_g)_{\perp}$,

$$(D_v-D)=-(9\pm3)\ \text{eV}\ ,$$

$$(D_\delta)_a=-(1.6\pm2.6)\ \text{eV}\ ,$$

$$(D_\delta)_b=(0.8\pm1.3)\ \text{eV}\ .$$

The diagram shows that the effect of crystallographic distortion associated with magnetic transition on $h\nu_g$ in MnO is

$$(D_v-D)(\Delta V/V)+D_\delta\,\delta$$
$$=(D_v-D)(\Delta V/V)+(D_\delta)_b\,\delta\ .$$

The value of $\Delta(E_1)_D+\Delta(E_2)_D$ calculated with $\Delta V/V$ and δ of crystallographic distortion is listed in Table I. The approximate value for α-MnS is calculated by using the same values of (D_v-D) and D_δ. The effect of magnetic transition on the localized state of excited electron in CoO is shown diagramatically at the bottom of Fig. 6. Magnetic transition is associated with contraction along a cubic axis instead of a ⟨111⟩ direction as in the Mn compounds. Symmetry distortion has no effect on the state of lowest energy, $(\psi_x+\psi_y+\psi_z)/\sqrt{3}$, i.e., $D_\delta=0$. The value of $\Delta(E_1)_D+\Delta(E_2)_D$ listed is estimated by using the (D_v-D) of MnO.

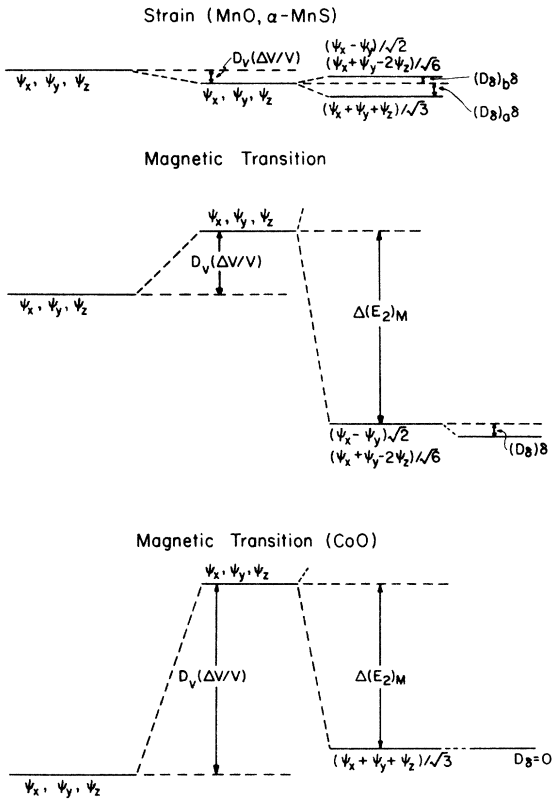

FIG. 6. Diagrams showing the effects of volume dilatation $\Delta V/V$, crystallographic distortion δ, and magnetic interaction $\Delta(E_2)_M$ on the energy legel of the optically excited electron, in the localized-electron model.

In the localized-electron model, $\Delta(E_2)_M$ is given theoretically by (25a) for Mn compounds and by (25b) for CoO. The values of $\Delta(E_2)_M$ listed in Table I require

$$2D^2 - E^2 = 0.09(J^0_{sd}/J_{sd}) \quad \text{for MnO},$$

$$2D^2 - E^2 = 0.03(J^0_{sd}/J_{sd}) \quad \text{for } \alpha - \text{MnS},$$

$$4D^2 + E^2 = 0.12(J^0_{sd}/J_{sd}) \quad \text{for CoO},$$

where J^0_{sd} is the s-d exchange integral for the free ion. $J^0_{sd} = 0.44$ eV (Ref. 29) for Mn^+. A similar method of estimation gives $J^0_{sd} = 0.49$ eV for Co^+. With $J^0_{sd}/J_{sd} \geq 1$, these conditions can be satisfied with reasonable values of D^2 and E^2. For example, with $J^0_{sd}/J_{sd} \simeq 2$, $2D^2 - E^2 = 0.18$ for MnO, $2D^2 - E^2 = -0.06$ for α-MnS, and $4D^2 + E^2 = 0.24$ for CoO. Referring to (24), it is seen that $8D^2$ is a measure of the contribution of the 4s orbitals of nearest magnetic ions and $2E^2$ pertains to the 4s orbitals of nearest magnetic ions and $2E^2$ pertains to the 4s orbitals of the next-nearest magnetic ions. For all three crystals, $8D^2 + 2E^2 \gtrsim 0.5$ is an indication that the contribution of p orbitals of the central ion and p orbitals of halogen neighbors is not too excessive. Furthermore, $8D^2 > 2E^2$ for all three crystals, which is consistant with a decrease of contribution of more distant ions. Finally, the fact that $2D^2 > E^2$ for MnO and $2D^2 < E^2$ for α-MnS seems to reflect the effect of a difference in dielectric constant: $K = 7.9$ for α-MnS and $K = 4.7$ for MnO. Therefore the wave function of localized electron may be expected to be more spread out in α-MnS.

---

†Work supported in part by a grant from Army Research Office, Durham, N.C.

[1]K. W. Blazey and H. Rohrer, Phys. Rev. 185, 712 (1969).
[2]G. Busch and P. Wachter, Phys. Kondens. Mater. 5, 232 (1966); Solid State Commun. 8, 1133 (1970).
[3]G. Busch, P. Junod, and P. Wachter, Phys. Lett. 12, 11 (1964); B. E. Argyle, J. C. Suits, and M. J. Freiser, Phys. Rev. Lett. 15, 822 (1965).
[4]G. Harbeke and H. Pinch, Phys. Rev. Lett. 17, 1090 (1966).
[5]G. Harbeke, S. B. Berger, and F. P. Emmenegger, Solid State Commun. 6, 533 (1968).
[6]H. W. Lehmann and F. P. Emmenegger, Solid State Commun. 7, 965 (1969).
[7]S. Wittekoek and P. F. Bongers, IBM J. Res. Dev. 14, 312 (1970).
[8]F. Rys, J. S. Helman and W. Baltensperger, Phys. Kondens. Mater. 6, 105 (1967).
[9]E. Callen, Phys. Rev. Lett. 20, 1045 (1968).
[10]R. J. Powell and W. E. Spicer, Phys. Rev. B 2, 2182 (1970).
[11]D. Adler and J. Feinleib, Phys. Rev. B 2, 3112 (1970).
[12]D. R. Huffman, R. L. Wild, and J. Callaway, J. Phys. Soc. Jap. 21, 623 (1966).
[13]Supplied by Nakazumi Crystal Corp., Japan.
[14]R. Nitsche, H. U. Bölsterli, and M. Lichtensteiger, J. Phys. Chem. Solids 21, 199 (1961).
[15]G. W. Pratt, Jr. and R. Coelho, Phys. Rev. 116, 281 (1959).
[16]D. R. Huffman, R. L. Wild, and M. Shinmei, J. Chem. Phys. 50, 4092 (1969).
[17]T. M. Wilson, Int. J. Quantum Chem. IIIS, 757 (1970).
[18]L. F. Mattheiss, Phys. Rev. B 5, 290 (1972).
[19]L. Messick, W. C. Walker and R. Glosser, Phys. Rev. B 6, 3941 (1972).
[20]G. K. Wertheim and S. Hüfner, Phys. Rev. Lett. 28, 1028 (1972).
[21]L. D. Finkel'shteyn and S. A. Newnonov, Fiz. Met. Metalloved. 32, 662 (1971) [Phys. Met. Metallogr. 32, 224 (1971)].
[22]D. Langer, J. Lumin. 1, 341 (1970).
[23]G. D. Mahan, J. Phys. Chem. Solids 26, 751 (1965).
[24]C. J. Ballhausen, *Introduction to Ligand Field Theory* (McGraw Hill, New York, 1962), Chap. 5.
[25]J. S. Griffith, *The Theory of Transition Metal Ions* (Cambridge U.P., Cambridge, England, 1961), p. 238.
[26]Y. Tanabe and S. Sugano, J. Phys. Soc. Jap. 9, 753, 766 (1954).
[27]D. M. Finlayson, I. S. Robertson, T. Smith, and R. W. H. Stevenson, Proc. Phys. Soc. Lond. 76, 355 (1960); F. W. Anderson, Solid State Phys. 14, 99 (1963).
[28]R. E. Watson and A. J. Freeman, Phys. Rev. 152, 566 (1966).
[29]J. Owen, M. Brown, W. D. Knight, and C. Kittel, Phys. Rev. 102, 1501 (1956).